Parametric studies of whispering-gallery mode resonators

Haiyong Quan[a], Zhixiong Guo[*a], Stanley Pau[b]
[a]Dept. of Mech. & Aerosp. Eng., Rutgers University, 98 Brett Road, Piscataway, NJ, USA 08854
[b]Nanofabrication Research Laboratory, Lucent Technologies/Bell Labs., Murray Hill, NJ, 07974

ABSTRACT

This report characterizes the whispering-gallery mode (WGM) resonators with the design of waveguide and microdisk coupling microstructure. In order to understand and optimize the design, studies over a broad range of resonator configuration parameters including the microdisk size, the gap separating the microdisk and waveguide, and the waveguide width are numerically conducted. The finite element method is used for solving the Maxwell's equations which govern the propagation of electromagnetic (EM) field and the radiation energy transport in the micro/nano-structured WGM systems. The EM field and the radiation energy distributions in the WGM resonator are obtained and compared between the on-resonance and off-resonance cases. A very brilliant ring with strong EM field and high radiation intensity is found inward the peripheral surface of the microdisk under the first-order resonance. While under the second-order resonance, there are two bright rings; and the outer ring inward the peripheral surface is thin and weaker than the internal ring. The microdisk size affects significantly the resonant frequencies and their intervals. The gap also has a slight effect on the resonant frequencies. The effect of waveguide width on the resonant frequencies is negligible. However, the gap as well as the waveguide width does obviously influence the qualify factor and the finesse of the resonant modes.

Keywords: Whispering-gallery mode, optical resonance, miniature sensor, waveguide, near-field optics, microcavity, finite element method, simulation, frequency shift, nanoscale detection.

1. INTRODUCTION

In recent years the advances in micro/nano-fabrication techniques have made it feasible to consider optical resonators having physical dimensions of the order of optical wavelengths. As a particular mode of microcavity resonances, the whispering-gallery mode occurs when light travels in a dielectric medium of circular geometry[1]. After repeated total internal reflections at the curvilinear boundary the electromagnetic field can close on itself, giving rise to resonances. The microcavity WGMs have recently received increasing attention due to their high potentials for the realization of microlasers[2], narrow filters[3], optical switching[4], optical biosensors[5], high resolution spectroscopy[6], etc.

WGM is a morphology-dependent resonance. Its resonant frequencies depend on the size of the resonator. In general, the resonant modes are approximately predicted by $2\pi r = mc_0/(f_m \cdot n)$, where m is integer, n is the refractive index of the resonator material, and r is the radius of the resonator. The frequency shift of a given resonant mode assuming constant refractive index is estimated as: $\Delta f / f \approx -\Delta r / r$, where Δr represents a small change of the radius. If we consider the linewidth of the resonance to be the smallest measurable shift (taken as $\Delta f = 10$ MHz, $f = 3.75\times10^8$ MHz at $\lambda = 800$ nm), then the smallest "measurable" size change is $|\Delta r|_{\min} = 2.6\times10^{-8} r$. With the radius $r \sim 10^4$ nm in typical miniature resonators, $|\Delta r|_{\min} = 2.6\times10^{-4}$ nm — a value smaller than the size of an atom!

Such a great trait can be explored for detection and sensing of adsorption or attachment of biological and chemical molecules to the peripheral surface of the resonator. When peptides, protein molecules, or cell membranes are attached on the resonator, for example, they interact with the evanescent field around the resonator. This interaction polarizes the

* guo@jove.rutgers.edu; phone 1 732 445-2024; fax 1 732 445-3124

Nanosensing: Materials and Devices, edited by M. Saif Islam, Achyut K. Dutta,
Proceedings of SPIE Vol. 5593 (SPIE, Bellingham, WA, 2004)
0277-786X/04/$15 · doi: 10.1117/12.571313

bio-molecules or cell membranes and changes the effective size of the resonator. This may lead to frequency shift of the resonance mode. Thus, it is possible to identify and detect bio-molecules by observing the resonant frequency shifts in a miniature WGM resonator. In recent years, WGM optical biosensors have been studied as a research field of attractive interest because of the great need in life sciences, drug discovery, and recent worldwide protection from the threat of chemical and bio-terrorism. Usually the optical resonance techniques can be used to enhance the sensitivity of biosensor devices[7]. The WGM miniature sensor possesses high sensitivity, small sample volume, and robust integrated property to make a lab-on-a-chip device[8] and can be used to identify and monitor proteins, DNA, and toxin molecules. They can detect as few as 100 molecules[9]. In many biosensing studies,[10,11] the WGM resonators are generally microstructures of a microsphere and an eroded optical fiber coupling design.

However, the microsphere and fiber coupling design has some obvious flaws for use as practical sensors. For instance, mass manufacture is difficult and non-uniformity exists; not to mention that it is difficult to control the gap distance between the eroded optical fiber and the microsphere which is critical for photon tunneling. In this study, we consider an innovative waveguide and microdisk coupling design as the WGM miniature resonator. In this design, mass manufacture can be easily achieved through nanofabrication, and the devices are of high uniformity and easy for calibration in factory. The new structure will further reduce the resonator size and enhance miniaturization. Figure 1 shows our design of the waveguide and microdisk coupling WGM resonator and a newly nanofabricated device using 248nm optical lithography and conventional silicon IC processing.

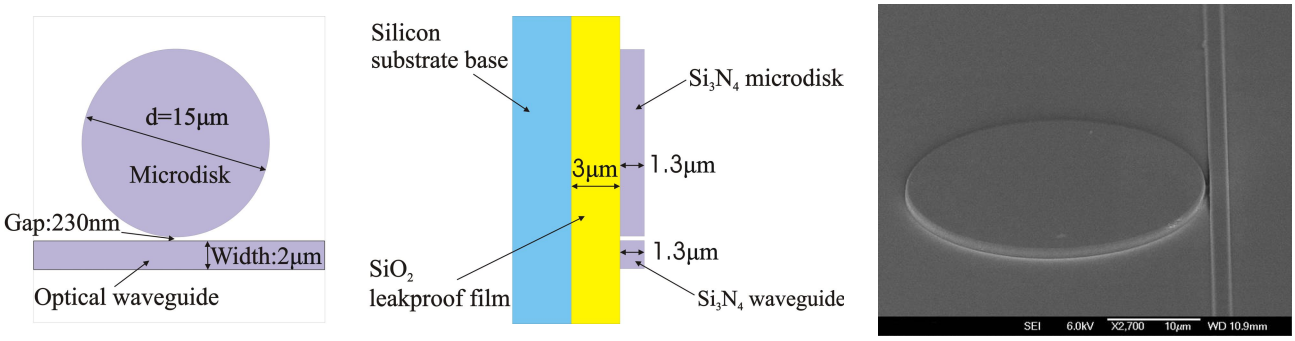

Figure 1. A WGM miniature resonator of waveguide and microdisk coupling design.

Parametric studies in simulation-based decision making are very useful for the optimal design of WGM resonators. In order to detect a specific molecule sensitively, the corresponding sensor configurations (e.g., the microdisk size, the gap between the microdisk and waveguide, and the waveguide size) and the operating laser wavelength range, need to be designed and optimized. The experimental method to optimize these parameters is very time-consuming and costly. A flexible simulation model is highly desired.

The optics in the WGM resonator involves far field and near field. Both the fields can be rigorously described by the Maxwell's electromagnetic (EM) theory. The Lorenz-Mie theory[12] and the first-order perturbation model[11] were previously used for analytical studies. The method of separation of variables[7] can also be utilized to solve the simplified Maxwell's equations - Helmholtz equation. The limitation of the theoretical models is that they can only be applied to reveal the individual intuitive resonance properties of the microcavity, but cannot expect to capture the coupling of the evanescent fields in the gap separating the microcavity and the waveguide. As a matter of fact, the signal strength in the microdisk is exponentially sensitive to the gap distance. Photon tunneling in the gap ensures the light transport from the waveguide to the microdisk. Further, the knowledge of light transport in the waveguide is critical for light delivery, signal collection, and material selection. A complete modeling of the whole EM field in the waveguide-microdisk micro/nano-structure is needed.

The Maxwell's equations can be solved by the finite-difference time-domain (FDTD) method[13]. The drawbacks of the FDTD method lie with the time consuming in obtaining stationary solutions, the large memory requirement, and the staircase approximation in the treatment of irregular configurations. Thus, it is not very ideal for simulation-based optimal design purpose. More than 30 years ago, Silcester[14] developed high order Lagrange elements and first applied

the finite element method (FEM) for solving the EM field problems. The first two authors[15] successfully applied the FEM to simulate the EM and radiation energy fields in the WGM resonators of microsphere and optical fiber coupling structure.

In this report, parametric studies through FEM simulations are made of the nano-opto-mechanical systems (NOMS) of the waveguide-microdisk coupling WGM resonators. The operating resonant frequencies are chosen in the near infrared range, which is ideal for biomaterials and biomolecules. The parameters selected for study include the diameter of the microdisk, the gap distance separating the waveguide and microdisk, and the width of the waveguide. Their effects on the WGM resonant phenomena will be scrutinized. The characteristics of the EM field and radiation energy storage in the WGM resonator under on-resonance and off-resonance will be investigated.

2. THEORY

WGM resonance inside the microdisk is typically an equatorial brilliant ring, and this ring is located on the same plane as the waveguide. So it is feasible to use a two-dimensional (2-D) theoretical model. The time-dependent Maxwell's equations are

$$\begin{cases} \nabla \cdot \bar{E} = \dfrac{\rho}{\varepsilon}; \quad \nabla \times \bar{E} = -\mu \dfrac{\partial \bar{H}}{\partial t} \\ \nabla \cdot \bar{H} = 0; \quad \nabla \times \bar{H} = \bar{J} + \varepsilon \dfrac{\partial \bar{E}}{\partial t} \end{cases} \tag{1}$$

where $\bar{E}$ and $\bar{H}$ are the electric and magnetic field vectors, respectively; ε and μ are the permittivity and permeability of the medium; ρ is the electric charge density; and $\bar{J}$ is the electric current density.

For the electric field, since $\rho = 0$ and $\bar{J} = \sigma \bar{E}$, we can derive the equation for $\bar{E}$ as follows:

$$\nabla^2 \bar{E} - \mu\sigma \frac{\partial \bar{E}}{\partial t} - \mu\varepsilon \frac{\partial^2 \bar{E}}{\partial t^2} = 0 \tag{2}$$

where σ is the electrical conductivity. We can transfer the above equation to the form of a time-harmonic wave by setting $\bar{E}(\bar{r},t) = \bar{E}_0(\bar{r})e^{i\omega t}$. The coupled set of Maxwell's equations is then reduced to a simple form:

$$\frac{1}{\mu}\nabla^2 \bar{E} + \omega^2 \varepsilon_c \bar{E} = 0; \quad \frac{1}{\mu}\nabla^2 \bar{H} + \omega^2 \varepsilon_c \bar{H} = 0 \tag{3}$$

where we have introduced the complex permittivity $\varepsilon_c = \varepsilon - i(\sigma/\omega)$ and $\omega = 2\pi c/\lambda$; c is the speed of light in the medium and λ is the light wavelength. Here, the complex index of refraction, $m = n - ik$, is conveniently introduced for the treatment of wave propagation; n is the real part of the refractive index and represents a spatial phase change of the electromagnetic wave; k is the absorption index and stands for a spatial damping on the electromagnetic wave. The relationship between ε_c and m is expressed by $\varepsilon_c = m^2 = n^2 - k^2 - i2nk$.

In the present study we consider the In-plane TE waves, where the electric field has only a *z*-component; and it propagates in the *x*-*y* plane. Thus, the fields can be written as:

$$\bar{E}(x,y,t) = E_z(x,y)\bar{e}_z e^{i\omega t}; \quad \bar{H}(x,y,t) = [H_x(x,y)\bar{e}_x + H_y(x,y)\bar{e}_y]e^{i\omega t}. \tag{4}$$

At the interface and physical boundaries, the natural continuity condition is used for the tangential component of the magnetic field, i.e., $\bar{n} \times \bar{H} = 0$. For the outside boundaries, the low-reflecting boundary condition is adopted. The low-reflecting means that only a small part of the wave is reflected, and that the wave propagates through the boundary almost as if it were not present. This condition can be formulized as $\bar{e}_z \cdot \bar{n} \times \sqrt{\mu}\bar{H} + \sqrt{\varepsilon}E_z = 0$. The light source term E_{0z}, which propagates inwards through the entry of the waveguide, was treated as an electrically low-reflecting boundary expressed by $\bar{e}_z \cdot \bar{n} \times \sqrt{\mu}\bar{H} + \sqrt{\varepsilon}E_z = 2\sqrt{\varepsilon}E_{0z}$.

The WGM resonances possess very high quality factors due to minimal reflection losses. The quality factor Q is defined as a ratio of 2π stored energy to energy lost per cycle. From the energy conservation and resonance properties, we can deduce a simple approximate expression:[16] $Q = \omega_0 / \Delta\omega = 2\pi\omega_0\tau$, where ω_0 is the resonant frequency, $\Delta\omega$ is the resonance linewidth, and τ is the photon lifetime.

The finite element method is employed to simulate the EM field and the details of the method are available in the papers by Quan and Guo[15,17]. Thus, the description is not repeated here. The commercial software FEMLAB was used for the finite element solution and for pre- and post-processing. A typical simulation model is similar to the left hand figure in Fig. 1. The simulation domain adopted is a 20μm × 25μm rectangular area with a centered microdisk. The length of the waveguide is extended to the edge of the simulation domain. A laser beam from a tunable continuous-wave (CW) laser is coupled into the left end of the waveguide to excite the resonance. The frequency of the incident laser varies between 365 THz (822nm) and 375 THz (800nm). In the nanometer scaled gap separating the waveguide and microdisk, photons tunnel and the light will cross the gap and enter into the microdisk. When the frequency of the input light is the same as the natural resonant frequency of the system, WGM phenomenon occurs. At the resonant frequency, the scattering intensity from the microdisk will increase sharply and form a peak in the intensity-frequency spectrum.

In the simulations, the model geometry is meshed by 51,400 triangle elements. The general computational resolution of wavelength is 0.5nm, but special attention is paid to the resonance frequencies where 0.01nm resolution is adopted. To conduct parametric studies, the diameter of the microdisk varies between 10 and 15μm. The width of the waveguide changes between 2 and 3μm. The gap between the microdisk and the waveguide varies between 100 to 300nm. Both the microdisk and the waveguide are made from silicon nitride (Si_3N_4) whose refractive index is 2.01 against the operating wavelength.

3. RESULTS AND DISCUSSION

3.1 Characteristics of the EM and energy fields of the WGM resonator

First we try to demonstrate the great difference of the EM field and radiation energy distributions between the on-resonance and off-resonance cases. Figures 2 and 3 illuminate the distributions of the electric field and the radiation energy, respectively. Three different cases under off-resonance, the first-order resonance, and the second-order resonance are selected for comparison. The first- and second-order resonance frequencies were found at 373.78 THz (λ=802.61nm) and 372.96 THz (804.37nm), respectively. The off-resonance frequency was selected at 372.67 THz (λ=805nm). The diameter of the microdisk was 15μm and the surrounding medium was air. The gap which is defined as the smallest distance between the waveguide and microdisk is 230nm and the width of the waveguide is 2μm.

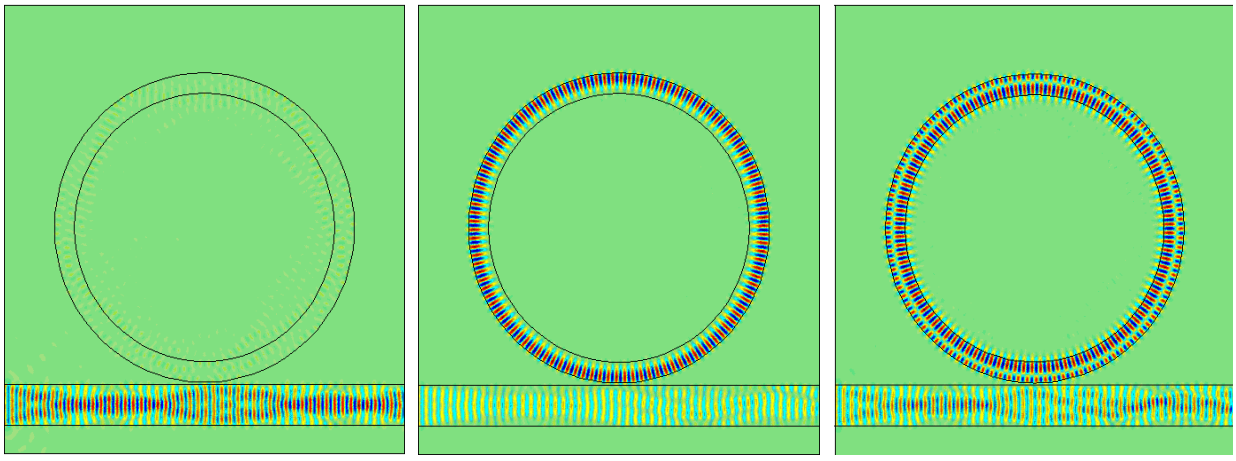

Figure 2. Electric field distributions under off-resonance, the first-order resonance, and the second-order resonance (from left to right).

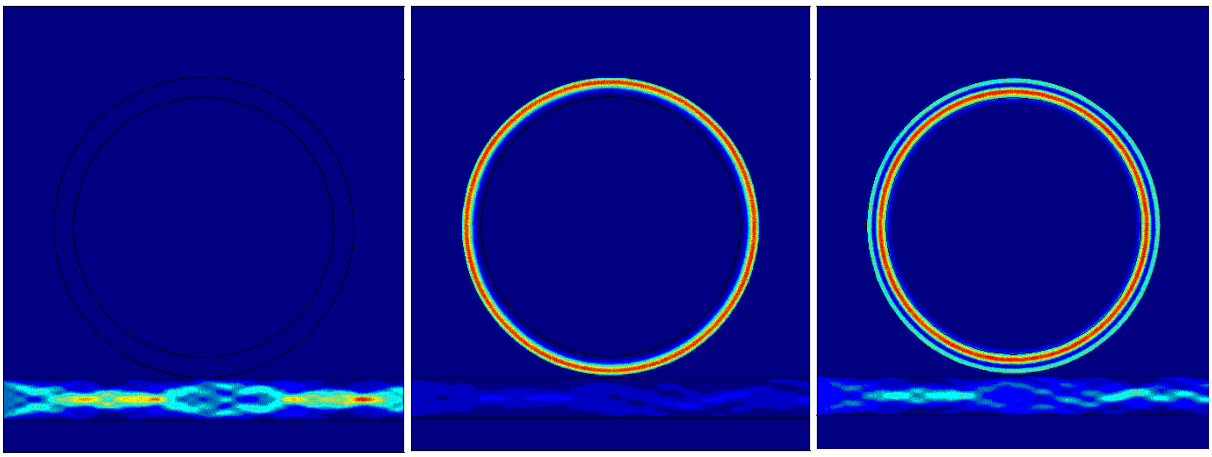

Figure 3. Energy distributions under off-resonance, the first-order resonance, and the second-order resonance (from left to right).

From Fig. 2, it is clearly observed that the EM field exists in the microdisk no matter there is a WGM resonance or no resonance. Thus, photons tunnel from the waveguide to the microdisk because the gap distance is less than one wavelength. Under the first-order resonance, a brilliant ring in the EM field is formed inside the microdisk in the vicinity close to the peripheral surface. While under the second-order resonance, there are two bright rings inside the microdisk. The EM field in the internal ring is stronger than that in the outer ring. For the EM field in the waveguide, however, the off-resonance case has the strongest strength and the first-order resonance case has the weakest strength.

From Fig. 3, it is seen that the microdisk and waveguide coupling resonator has a very strong energy storing property in the resonator when WGMs occur. The majority energy stores in the thin ring close to the peripheral surface of the microdisk for the first-order resonance. For the second-order resonance, the energy is mostly stored in the internal ring. However, there still exists an outer ring which is thin and weak as compared with the internal ring. Thus, the scattering intensity from the microdisk surface under the second-order resonance is expected to be weaker than that under the first-order resonance. For the case of off-resonance, the energy is confined inside the waveguide and energy storage in the resonator is almost invisible. The ratio of the radiation energy storing in the microdisk to the radiation energy passing through the waveguide is 10.5 for the first-order resonance shown in Fig. 3, whereas it is only 0.008 for the case of off-resonance. The microdisk can absorb and store the majority of the radiation energy when WGM resonance occurs. This leads to the enhancement of radiation field around the periphery of the resonator, where sensitivity to any external perturbation is maximal.

Compared with the EM field and energy distribution results in our previous study[17] for WGM resonators with a microsphere and eroded optical fiber coupling structure, we found that the new design of waveguide-microdisk coupling resonator has greatly improved the quality of WGM resonances. The ratio of the radiation intensity storing in the microsphere to the radiation intensity passing through the optical fiber was only 1.8 at resonance in our previous study.

3.2 Parametric studies

The resonator configuration like the microdisk size, the gap between the waveguide and microdisk, and the width of the waveguide certainly affects the resonance phenomena and signal intensity. To investigate the parametric influences, we obtained the scattering spectra of radiation energy outflow (Poynting's vector from the microdisk peripheral surface) with varying excitation frequencies between 365 THz and 375 THz for different microdisk diameters, gap distances, and waveguide widths, respectively. Figure 4 shows the scattering spectra for three different microdisk diameters: 10μm, 12.5μm, and 15μm. The width of the waveguide and the gap between the waveguide and microdisk are fixed at 2μm and 230nm, respectively. The resonance data retrieved from these scattering spectra are listed in Table 1. The parameters include the resonant frequency and its corresponding wavelength, the quality factor, the full-width at half maximum (FWHM) of the resonant frequency band, the resonant frequency interval represented by the free-spectral range (FSR, = periodicity of resonance peaks), and the finesse of the resonant mode defined as F = FSR/FWHM. Three first-order resonant frequencies (modes) were found for each of the cases in the frequency range considered.

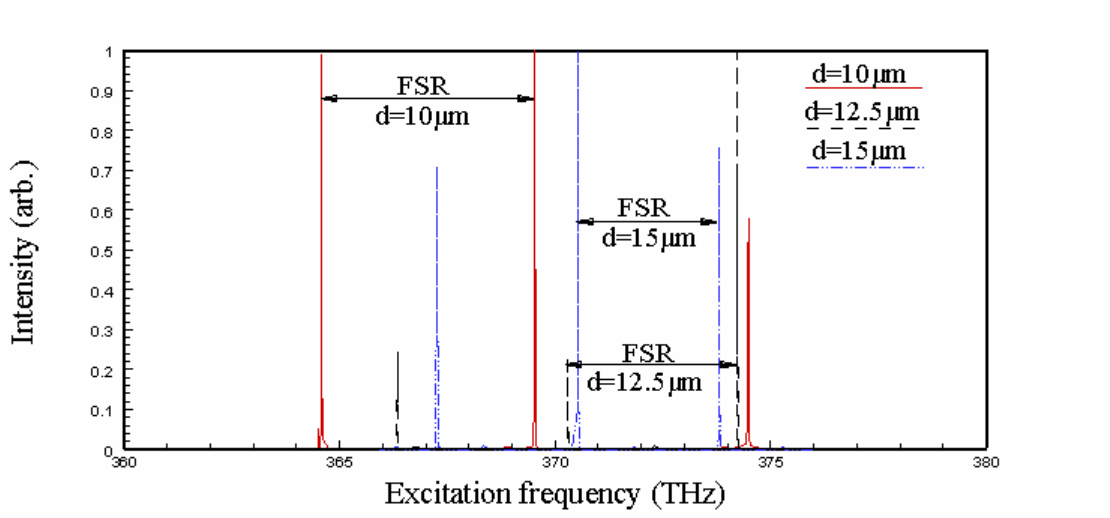

Figure 4. Scattering spectra for different microdisk sizes of d = 10μm, 12.5μm, and 15μm, respectively.

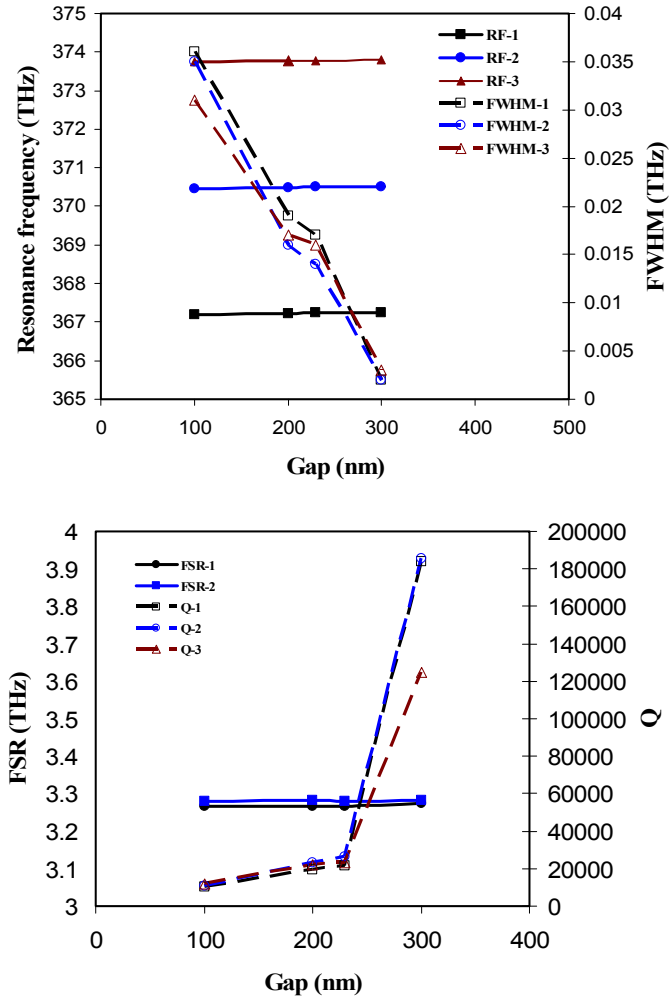

Figure 5. Effects of the gap on the WGM resonant frequencies, FWHM, FSR, and quality factor Q.

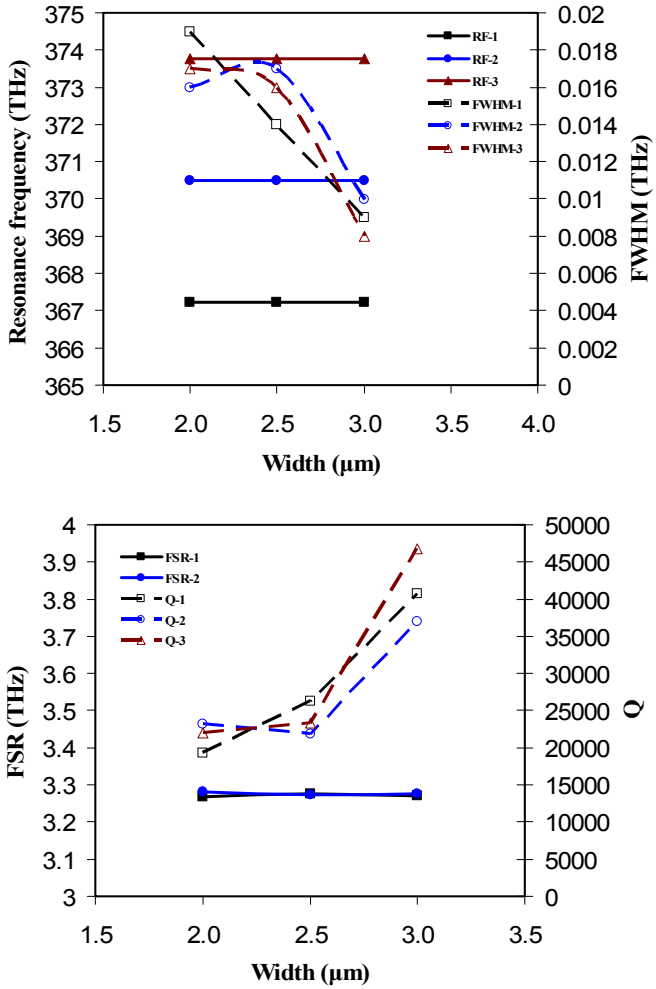

Figure 6. Effects of the waveguide width on the WGM resonant frequencies, FWHM, FSR, and quality factor Q.

Since both the gap and waveguide width do not affect the resonance modes, it is not easy to find differences in the scattering spectra for different gap distances and waveguide widths. Figures 5 and 6 portray the gap and waveguide width effects, respectively, on the WGM resonant frequencies, the corresponding FWHM and FSR, and the quality factor Q. All the data were retrieved from the respective scattering spectra and are listed in Table 1. Four different gap distances of 100nm, 200nm, 230nm, and 300nm, and three different waveguide widths of 2.0μm, 2.5μm, and 3.0μm were considered. The surrounding medium was air for all simulation conditions. There are three whispering-gallery modes (RF-1, RF-2, and RF-3) in the frequency range considered, and each mode has its own FWHM and Q values.

From Figs. 4 to 6 and Table 1, it is found that the microdisk size affects significantly the resonant frequencies and their intervals. The FSR value increases with the decrease of the diameter of the microdisk. However, the microdisk size does not appreciably influence the quality factor and the finesse. On the other hand, the gap and the waveguide width do strongly affect the quality factor and the finesse of the WGM. But the gap has a slight effect on the resonant frequencies and the FSR, and the influence of the waveguide width on the resonant frequencies and the FSR is negligible. The decrease of the gap results in a broadening in the FWHM of the resonant frequency band, and consequently reduces the quality factor and the finesse of the resonant frequencies. The wider is the waveguide, the larger are the quality factor and the finesse of the resonant modes. The quality factors of these resonant modes are varying between 10,200 and 185,255 in the present studies. The finesse of these resonance modes is in a range from 92.0 to 1637.5. The FSR of the resonant modes for the 15μm-diameter microdisk are slightly varying between 3.266 THz and 3.281 THz for all the

specified gap distances and waveguide widths. Thus, the WGM frequencies are dominantly determined by the microdisk diameter. The gap distance and the waveguide width affect mainly the resonance quality.

Table 1. Resonance data from the scattering spectra.

Resonance frequency f_R (THz)	Excitation Wavelength λ_R (nm)	Quality factor Q	FWHM (THz)	FSR (THz)	Finesse F
d = 10.0μm, g = 230nm, w = 2.0μm					
364.582	822.86	21,446	0.017	4.944	282.5
369.526	811.85	20,529	0.018		
374.490	801.09	22,029	0.017	4.964	283.6
d = 12.5μm, g = 230nm, w = 2.0μm					
366.321	818.53	22,895	0.016	3.931	253.6
370.252	810.26	24,683	0.015		
374.201	801.71	22,011	0.017	3.949	246.8
d = 15.0μm, g = 230nm, w =2.0μm					
367.235	816.92	21,602	0.017	3.266	210.7
370.501	809.72	26,464	0.014		
373.780	802.61	23,361	0.016	3.279	218.6
d = 15.0μm, g = 100nm, w = 2.0μm					
367.197	817.00	10,200	0.036	3.267	92.0
370.464	809.79	10,585	0.035		
373.743	802.69	12,056	0.031	3.279	99.4
d = 15.0μm, g = 200nm, w = 2.0μm					
367.224	816.94	19,328	0.019	3.267	186.7
370.495	809.73	23,155	0.016		
373.776	802.63	21,987	0.017	3.281	198.8
d = 15.0μm, g = 300nm, w = 2.0μm					
367.235	816.91	183,617	0.002	3.275	1,637.5
370.510	809.70	185,255	0.002		
373.791	802.59	124,597	0.003	3.281	1,312.4
d = 15.0μm, g = 200nm, w = 2.5μm					
367.215	816.96	26,230	0.014	3.277	211.4
370.492	809.73	21,794	0.017		
373.765	802.64	23,360	0.016	3.273	198.4
d = 15.0μm, g = 200nm, w = 3.0μm					
367.217	816.96	40,802	0.009	3.271	344.3
370.488	809.74	37,049	0.010		
373.764	802.65	46,721	0.008	3.276	364.0

4. CONCLUSIONS

The characteristics of waveguide-microdisk coupling WGM miniature resonators were studied based on the computer simulations. The time-dependent Maxwell's equations were utilized for describing the propagation and transport of the EM field from micrometer scale to nanometer scale in the micro/nano-structured WGM resonators. The finite element method was useful in the solution of the Maxwell's equations with irregular geometries. The EM field and the radiation energy distribution in the resonators were obtained. It is found that photon tunneling between the waveguide and microdisk exists no matter WGM resonance occurs or not. However, the tunneling is very weak under off-resonance conditions and the radiation energy is well confined inside the waveguide. When WGM resonance occurs, photon tunneling is greatly enhanced and significant radiation energy is stored in the microcavity. In the case of first-order resonance, the radiation energy in the microdisk could be 10 times higher than that passing through the waveguide; a very brilliant ring with strong EM field and high radiation intensity is found inward the peripheral surface of the microdisk. Under the second-order resonance, there are two bright rings inside the microdisk; and the strength of the outer ring is weaker than that of the internal ring. This explains why the strength of the first-order resonance in the scattering spectra is more appreciable and the first-order resonance frequencies are usually utilized for measuring frequency shifts. Parametric studies are made of a broad range of parameter values of the microdisk size, the gap separating the microdisk and waveguide, and the waveguide width. The WGM resonant frequencies and their intervals are mainly determined by the microdisk diameter. The gap separating the waveguide and microdisk and the waveguide size have little effect on the resonant frequencies and their intervals. However, the gap as well as the waveguide width does strongly influence the qualify factor and the finesse of the resonant modes.

ACKNOWLEDGMENTS

Z. Guo acknowledges the partial support of a 2003 - 2004 Academic Excellence Fund Award from Rutgers University and a NSF grant (CTS-0318001) to the project. The sponsor of device fabrication from the New Jersey Nanotechnology Consortium is also appreciated.

REFERENCES

1. S. Arnold, "Microspheres, photonic atoms and the physics of nothing", *American Scientists*, **89**, 414-421 (2001).
2. M. Cai, Q. Painter, K.J. Vahala, and P.C. Sercel, "Fiber-couppled microsphere laser", *Opt. Lett.*, **25**, 1430-1432 (2000).
3. B.E. Little, S.T. Chu, H.A. Haus, J. Foresi, and J.P. Laine, "Microring resonator channel dropping filters", *J. Lightwave Tech.*, **15**, 998-1005 (1997).
4. F.C. Blom, D.R. van Dijk, H.J Hoekstra, A. Driessen, and T.J.A. Popma, "Experimental study of integrated-optics micro-cavity resonators: toward an all-optical switching device," *Appl. Phys. Lett.*, **71**, 747-749 (1997).
5. R.W. Boyd, and J.E. Heebner, "Sensitive disk resonator photonic biosensor", *Appl. Opt.*, **40**, 5742-5747 (2001).
6. S. Schiller, and R.L. Byer, "High-resolution spectroscope of whispering gallery modes in large dielectric spheres," *Opt. Lett.*, **16**, 1138-1140 (1991).
7. S. Blair and Y. Chen, "Resonant-enhanced evanescent-wave fluorescence biosensing with cylindrical optical cavities", *Appl. Opt.*, **40**, 570-582 (2001).
8. F. Vollmer, D. Braun, A. Libchaber, M. Khoshsima, I. Teraoka, and S. Arnold, "Protein detection by optical shift of a resonant microcavity", *Appl. Phys. Lett.*, Vol. 80, No. 21, pp. 4057-4059 (2002).
9. R.W. Boyd, and J.E. Heebner, "Sensitive disk resonator photonic biosensor", *Appl. Opt.*, **40**, 5742-5747 (2001).
10. S. Arnold, M. Khoshsima, I. Teraoka, and F. Vollmer, "Shift of whispering-gallery modes in microspheres by protein adsorption", *Opt. Lett.*, **28**, 272-274 (2003).
11. I. Teraoka, S. Arnold, and F. Vollmer, "Perturbation approach to resonance shifts of whispering-gallery modes in a dielectric microsphere as probe of a surrounding medium", *J. Opt. Soc. Am. B*, **20**, 1937-1946 (2003).
12. P.W. Barber and P.K. Chang, *Optical effects associated with small particles*, World Scientific, Singapore; New Jersey; Hong Kong (1988).
13. A. Taflove and S.C. Hagness, *Computational Electrodynamics: The Finite-Difference Time-Domain Method*, 2nd ed., Artech House, Norwood, MA (2000).
14. P.P. Silvester, "Finite element solution of homogeneous waveguide problems", *Alta Frequenza*, **38**, 313-317 (1969).

15. H. Quan and Z. Guo, "Finite element analyses of near-field radiation and resonance frequency shift in WGM nanoscopic biosensors," *Heat Transfer Science and Technology* 2004 (Bu-Xuan Wang Ed.), pp. 101 – 108, Proc. of *the 6th International Symposium on Heat Transfer*, Beijing, China, June 15-19, 2004.
16. A. Yariv, *Optical electronics in modern communications*, 5th ed., Oxford U. Press, Oxford, UK (1997).
17. H. Quan and Z. Guo, "Simulation of whispering-gallery-mode resonance shifts for optical miniature biosensors", *J. Quantitative Spectroscopy & Radiative Transfer*, in press (2004).